General Disclaimer

One or more of the Following Statements may affect this Document

- This document has been reproduced from the best copy furnished by the organizational source. It is being released in the interest of making available as much information as possible.

- This document may contain data, which exceeds the sheet parameters. It was furnished in this condition by the organizational source and is the best copy available.

- This document may contain tone-on-tone or color graphs, charts and/or pictures, which have been reproduced in black and white.

- This document is paginated as submitted by the original source.

- Portions of this document are not fully legible due to the historical nature of some of the material. However, it is the best reproduction available from the original submission.

A.R.A.P.

AERONAUTICAL RESEARCH ASSOCIATES of PRINCETON, INC.

A.R.A.P. Report No. 494

Range Safety Signal Attenuation by the Space
Shuttle Main Engine Exhaust Plumes

Period 27 August 1982 to 25 January 1983

19 April 1983

NAS8-34956

Blaine E. Pearce

Aeronautical Research Associates of Princeton, Inc.
50 Washington Road, P.O. Box 2229
Princeton, New Jersey 08540

Prepared for
George C. Marshall Space Flight Center
Marshall Space Flight Center
Alabama 35812

CONTENTS

ABSTRACT

An analysis of attenuation of the Range Safety Signal at 416.5 MHz observed after SRB separation and ending at hand over to Bermuda, during which transmission must pass through the LOX/H_2 propelled main engine exhaust plumes, is summarized. Absorption by free electrons in the exhaust plume can account for the nearly constant magnitude of the observed attenuation during this period; it does not explain the short term transient increases that occur at one or more times during this portion of the flight. It is necessary to assume that a trace amount (about 0.5 ppm) of easily ionizable impurity must be present in the exhaust flow. Other mechanisms of attenuation, such as scattering by turbulent fluctuations of both free and bound electrons and absorption by water vapor, were examined but found to be inadequate to explain the observations.

ACKNOWLEDGEMENTS

NOMENCLATURE

A	Nozzle area
B	Constant in plume density equation
C_F	Nozzle thrust coefficient
c	Speed of light
k	Wavenumber ($= 2\pi/\lambda$)
$\ell*$	Characteristic plume length $\left[= (T/q_\infty)^{1/2}\right]$
M_∞	Flight Mach number
$\overline{M}$	Mean molecular weight
n	Molecular number density
n_p	Plasma index of refraction
$\overline{n'^2}$	Mean square fluctuation in index of refraction
p	Pressure
q_∞	Freestream dynamic pressure
Q	Scattering efficiency
R	Amplitude reflection coefficient
s	Distance along line-of-sight
T	Temperature, K, or thrust
t	time
α	Attenuation constant for absorption by free electrons
α_s	Attenuation constant for scattering by turbulence
α_{H_2O}	Attenuation constant for absorption by water vapor
β	Phase constant, or $1 - \cos\theta$ in plume density equation
θ	Angle of incidence of a plane wave
Λ	Turbulence macroscale length, or constant in plume density equation
λ	Wavelength
μ_i	Species mole fraction
ν	Circular frequency
ν_{en}	Electron-neutral collision frequency
ρ	Mass density
ϕ	Angle between line-of-sight and plume axis (aspect angle $= \pi-\phi$)
ω	Radian frequency

Subscripts

CL	Centerline
c	Chamber
e	Exit plane, or electron
o	Reference conditions

Superscript

*	Conditions at the nozzle throat

1.0 INTRODUCTION

The Space Shuttle has a Range Safety System (RSS) that can terminate the thrust and separate the two solid rocket boosters (SRB's) from the Orbiter and also separate the external tank (ET) from the Orbiter in an emergency. The commands for these events are transmitted from the ground by means of an FM-frequency shift keyed signal with a center frequency of 416.5 MHz. It is a requirement that this signal never drop below 81 dBm.

Previous analyses (Boynton, et al., 1977, 1978) and measurements show that severe interference and attenuation occur during the SRB burn. This was expected because of the composition of the solid propellant. It contains impurities such as sodium (Na), potassium (K), and chlorine (Cl) that are easily ionized and contribute to a large number density of free electrons in the motor exhaust plumes. These propellants also burn at conditions that provide a fuel-rich exhaust (excess carbon monoxide and hydrogen) that allows subsequent combustion (afterburning) when the exhaust mixes with air to further increase the temperature and electron concentration over their values at the nozzle exit.

Subsequent to separation of the SRB's, the exhaust plume is due only to the three liquid oxygen-hydrogen (LOX/H_2) main engines. This oxidizer-fuel combination is known to have a very clean exhaust which is expected to be nominally free from impurities that can contribute free electrons at the temperature levels experienced by the gases (< 3600 K). Pre-flight estimates of the RSS signal do not even consider any attenuation from these plumes.

However, comparisons of the predicted and measured RSS signal indicate an attenuation during that portion of the trajectory subsequent to SRB separation when the transmitter line-of-sight passes through the main engine exhaust plumes and vehicle wake. The essential features of this attenuation are (see Figure 1):

1. it occurs after SRB separation (t ~ 127 sec) to the time of hand over to Bermuda (t ~ 430 sec),

2. the line-of-sight from the Cape Command transmitter to the Orbiter during this period varies from about 20° to 10° from tail-on (160-170° from nose-on). At hand over to Bermuda, the aspect angle changes to near nose-on.
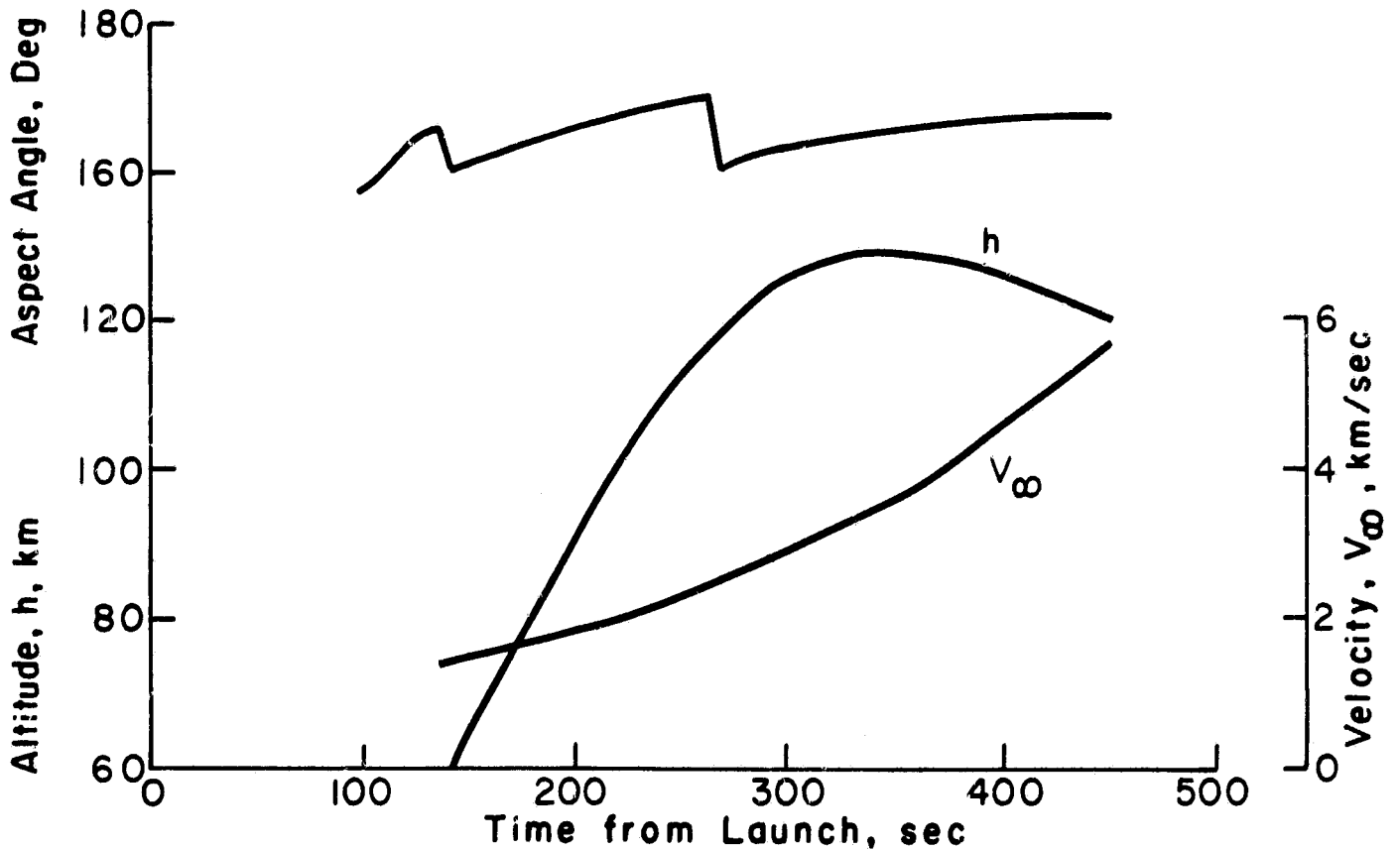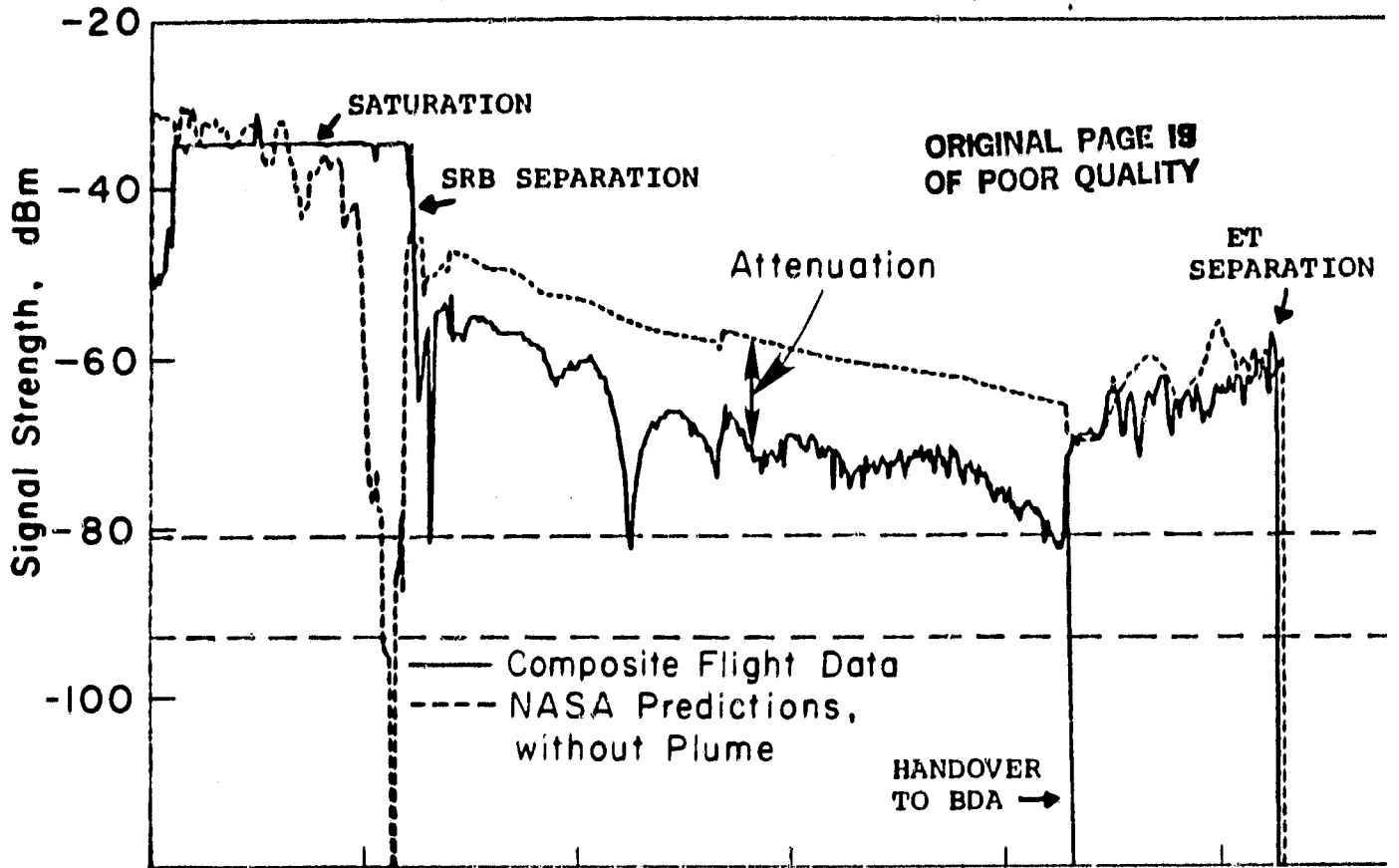
Figure 1. Observed Attenuation and Trajectory Parameters for STS-2.

3. the attenuation level changes slowly from near 5 dB to at most 15 dB with increasing time between 127-430 sec after launch. There are times between 200 and 300 sec where the attenuation increases suddenly and then decreases again within a short period of 10-20 sec. This additional attenuation is superposed on the nominal level which slowly increases with time.

4. the attenuation is repeatable; the overall levels and peaks are about the same for STS flights 2, 3, 4, and 5, although the times at which the peaks occur differs from flight to flight. (No measurements were made for the STS-1.)

5. during this period, the vehicle altitude increases from about 53 to 130 km, and the velocity increases from about 2.0 to 6.0 km/sec.

The aspect angle dependence and repeatability suggest a plume and/or wake related cause for the unexpected attenuation. However, the source of the attenuation, unlike that of the SRB plumes, is not obvious. It is argued that the repeatability rules out an explanation based on atmospheric effects because the launches were at different times of the year. There is the possibility that there may be a reason unrelated to any gas dynamics origin, such as a systematic error in the gain pattern of the RSS antenna on the ET. However, that possibility is not considered to be a likely explanation.

This unexplained attenuation is not a critical issue at this time. For these first five flights, the opinion is that the RSS would have operated if needed. Launch azimuths for subsequent flights are such that no additional attenuation is expected. However, the Space Shuttle is a manned vehicle with the potential for a wide variety of missions that may require launch situations other than those contemplated for the near future. It is therefore desirable to understand the reasons for this unknown attenuation, in order to determine if there are lines-of-sight, altitudes, and velocities for which the attenuation might be sufficient to compromise the RSS operation.

This report summarizes an analysis which attempts to determine if there are plume and/or wake related phenomena that can explain the observed attenuation during the period when only the LOX/H$_2$ main engines are operating. The properties of the exhaust plume and wake are examined to determine if they can contribute RF attenuation of the magnitude needed to explain the measurements.

2.0 PRELIMINARY ASSESSMENTS

2.1 Plume and Wake Flowfields

It is important to acknowledge at the beginning that a precise prediction of the Space Shuttle exhaust plume structure is not possible because there are three engines involved. Moreover, the same limitation exists for the vehicle wake because of the complicated shape of the Orbiter and because of the attached external tank. These limitations are particularly important in the nearfield where the disturbed flow has not yet relaxed to a uniform ambient pressure. A simple estimate of the plume length that affects the attenuation can be obtained from the range of aspect angles encountered. For example, aspect angles from 10-20 degrees from tail-on imply lines-of-sight that are affected by plume lengths of from 1.0-2.5 $\ell*$, where $\ell* = (T/q_\infty)^{1/2}$ is a characteristic scaling length for which high altitude plume shapes become similar (Moran, 1974). In actual dimensions, these lengths are from 0.15 to 13 km for the altitudes and velocities of interest. These dimensions are large, but the plume and wake flows are not yet equilibrated to ambient pressure. Both the plume and wake still retain a sensitivity to the initial conditions of the flow over the vehicle, which are not accurately known.

An additional restriction is that the altitudes of interest are high (> 53 km). Our current detailed exhaust plume and wake numerical codes are not applicable at altitudes above about 70 km (Dash, et al., 1980), and so more approximate calculations must be used. However, for this particular study, the upper limit for these codes was found to be 80 km.

2.2 Identification of Easily Ionizable Species

An essential part of this study was the identification of the presence of ionizable species in the plume and wake that could generate free electrons. A survey of the oxidizer and fuel of the main engines was made with the result than no species of this type could be identified. Consequently, there are no easily ionizable species known to be in the main engine exhaust. The known source of these species in the ET ablation products is quickly exhausted. A conclusion from this assessment is that there is no a priori identifiable source of free electrons in the plume or wake that offers a potential explanation.

There is a source of free electrons in the partially ionized air that passes through the shock wave of the vehicle and plume. This source is confined to the outer edges of the plume and will be examined subsequently.

Because of this initially negative result of no easily identifiable ionizable species, the study was forced to take essentially an inverse approach. That is, the analysis works backwards from the known level of attenuation to determine what amount and origin of trace impurities are required to offer a possible explanation.

2.3 Catalogue of Possible Attenuation Mechanisms

Before presenting the details of the analyses, a list of the gas dynamic phenomena that could contribute RF attenuation is presented. Each is listed in Table 1 and roughly identified by its origin and spatial location in the flow.

3.0 ATTENUATION BY EXHAUST PLUME

3.1 Initial Conditions

For the purpose of this study, the exhaust plumes from the three main engines were combined into an equivalent plume from a single engine with the total exit area. Exit plane properties were obtained by a one-dimensional flow solution from the chamber conditions. The exit plane conditions are summarized in Table 2.

An important result of these calculations is that trace species in the exhaust, e^-, OH, OH^-, etc. are chemically frozen near the nozzle throat. This result is particularly important for any ionizable species that might be present. A sample kinetic calculation for the electron mole fraction in the nozzle resulting from a contamination level of 1 ppm of Na ($\mu_{Na} = 10^{-6}$) is shown in Figure 2. Because of the expansion, the electron concentration is frozen at near its chamber value with the result that the concentration at the exit plane is much larger than it would be under equilibrium conditions. Major species in the nozzle flow (H_2O and H_2) are essentially in equilibrium. Initial conditions for the subsequent plume expansion were taken from the chemical kinetics calculations.

TABLE 1.   SUMMARY OF RF ATTENUATION MECHANISMS EXAMINED

Gas Dynamic Region	Attenuating Species	Mechanism of Attenuation	Spatial Location
exhaust plume core	ionizable species in exhaust	absorption by free electrons	inviscid core of plume
	water vapor	microwave absorption	inviscid core of plume
wake, plume mixing layer	ionized species in exhaust, ablation products, shock heated air	absorption by free electrons	plume boundary
	ionized species in exhaust, ablation products, shock heated air	scattering by fluctuations in electron concentrations	plume boundary
		reflection of incident wave	plume boundary
	water vapor, carbon dioxide, nitrogen oxygen molecules	scattering by fluctuating index of refraction	plume boundary

TABLE 2. EXIT PLUME PROPERTIES OF MAIN ENGINE

(a) Chamber Conditions

   LOX/H_2 with Oxidizer/Fuel = 6.0
   P_c = 204.9 atm
   T_c = 3616 K
   $A_e/A*$ = 78.5

(b) Exit Plane Properties

   Exit Temperature, 1183 K
   Exit Pressure, 0.1773 atm
   Exit Velocity, 4488 m/sec
   Exit Lip Angle 10°
   Effective Exit Radius, 1.98 m

Exit Plane Composition:

Species	Mole Fraction	Species	Mole Fraction
e^-	2.46(-10)	NaO	---
H	5.55(-4)	NaOH	8.10(-10)
H_2	2.67(-1)	O	1.24(-3)
H_2O	7.27(-1)	O^-	---
HO_2	---	OH	2.70(-3)
H_2O_2	---	OH^-	3.31(-9)
Na^+	3.83(-9)	O_2	1.64(-3)
Na	1.01(-9)	O_2^-	---

NOTES:
(1) Includes 1 ppm Na as a model of a trace amount of easily ionizable impurity.

(2) Species list includes all those formed in chamber.

(3) All quantities except exit plane composition were determined by chemical equilibrium rocket motor performance code (Gordon and McBride, 1976).

(4) Non-equilibrium composition was calculated with a one-dimensional, stream tube code.

$p_c = 204.9$ atm
$T = 3616$ K
$O/F = 6$

ARAP 83-2231

kinetic

equilibrium
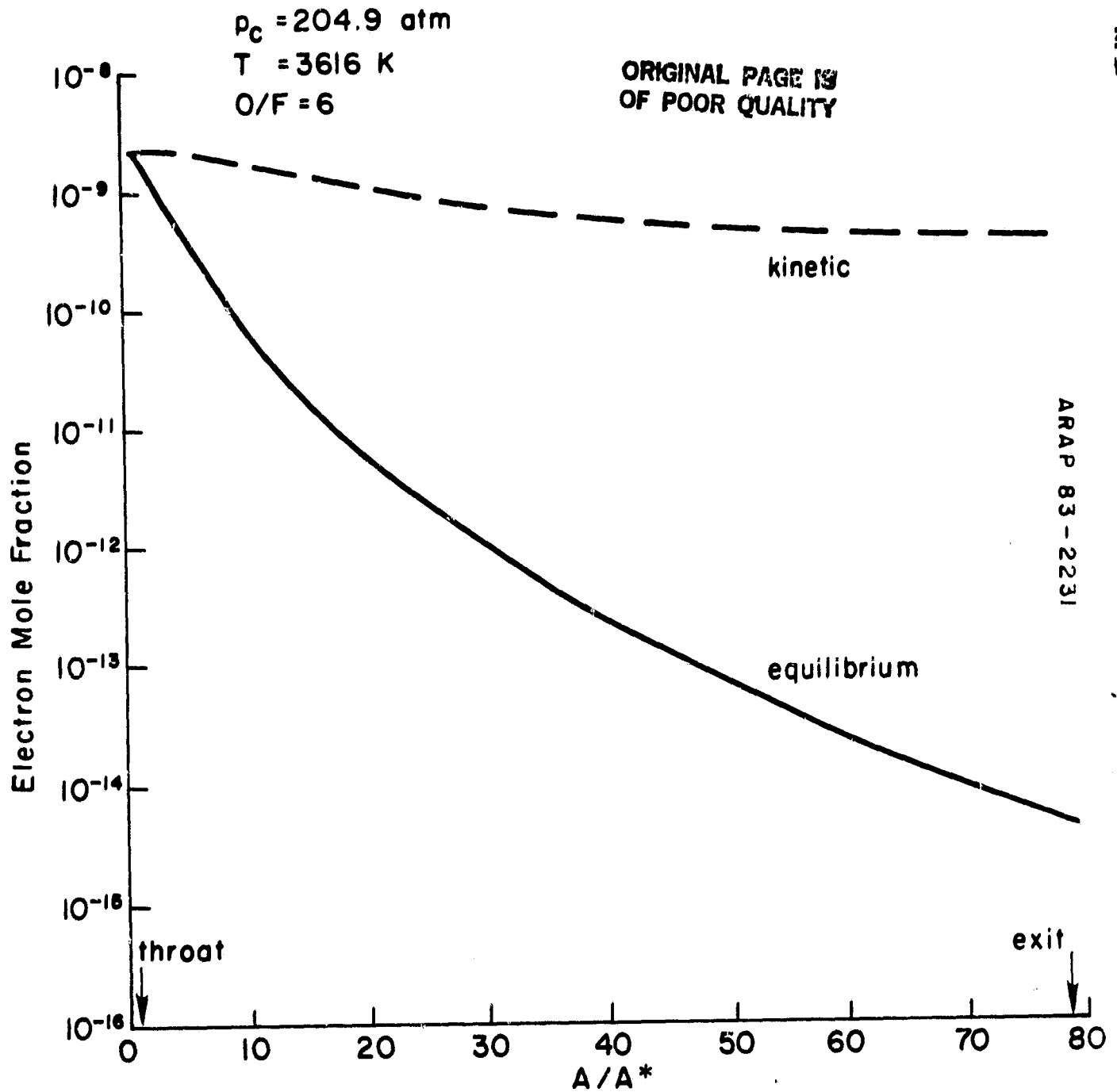
throat

exit

A/A*

Electron Mole Fraction

Figure 2. Electron Concentration in Nozzle for an Equilibrium and
Chemical Kinetic Controlled Expansion. Assumed 1 ppm
of Na as an Impurity.

3.2 Plume Structure

Subsequent to the nozzle exit, the flow expands even farther because of the low ambient pressure ($p_\infty/p_e \ll 1$). Calculations accounting for the detailed chemical kinetics of the exhaust gases show that the chemistry at these altitudes is very slow beyond the exit plane, afterburning of the excess H_2 is suppressed, and the entire plume composition is frozen at the nozzle exit conditions.

The nearfield plume structure, accounting for the inviscid expansion and turbulent mixing* of the plume with the atmosphere was calculated with A.R.A.P.'s version of the JANNAF Standard Plume Model (SPF/1) (Dash, et al., 1980). Although this code is nominally operable to about 70 km, solutions up to 80 km altitude were obtained for the Shuttle main engines. A sketch of the inviscid plume boundary and superposed mixing layer is given in Figure 3. These solutions were obtained between altitudes of 60 and 80 km and were used for the basic detailed attenuation predictions. However, because of this altitude limitation, arguments about the attenuation at higher altitudes are based on approximate plume models and scaling relations.

The overall inviscid structure of high altitude plumes becomes self-similar if the dimensions are normalized by $\ell^* = (T/q\infty)^{1/2}$. In the present case, T is the total thrust of the three engines (3×470 klb$_f$ = 6.27×10^6 N). This scaling is verified at the lower altitudes of interest by the detailed calculations used here. The scaled plumes are shown in Figure 4. For aspect angles of 10-20 degrees from tail-on, the attenuation by the plume and/or wake is contributed by the nearfield where the inviscid structure determines the plume shape, except for the mixing layer between the plume and freestream gases.

3.3 Primary Attenuation Mechanisms

With the detailed plume flowfield and chemical composition prescribed, attenuation predictions for the appropriate lines-of-sight were performed with the Naval Weapons Center Plume Radar Frequency Interference Code (PRFIC) (Pearce and McCullough, 1982). For a given flowfield, geometry of observation, and radar frequency, this code predicts the attenuation due to absorption and scattering by the mean and fluctuating free electron number density.

---

*even though the flow is a high altitude, low density plume, the flow is still turbulent throughout the portion of the trajectory of interest here.

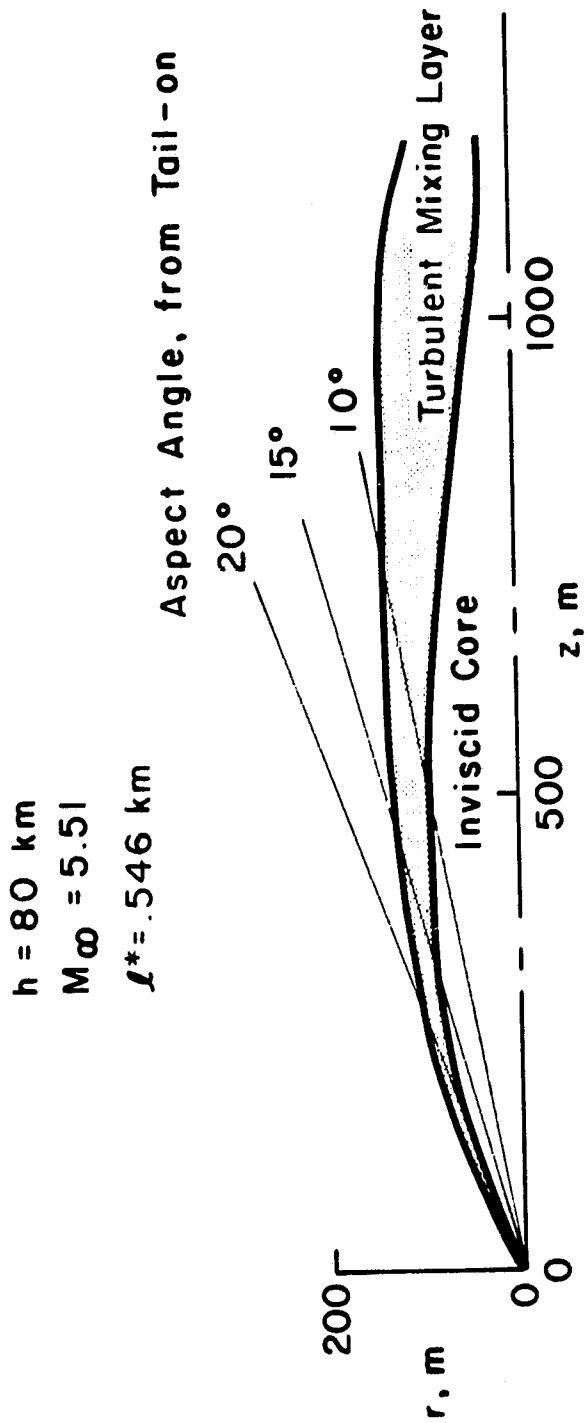Figure 3. Exhaust Plume Structure for Equivalent Shuttle Plume at 80 km Altitude.

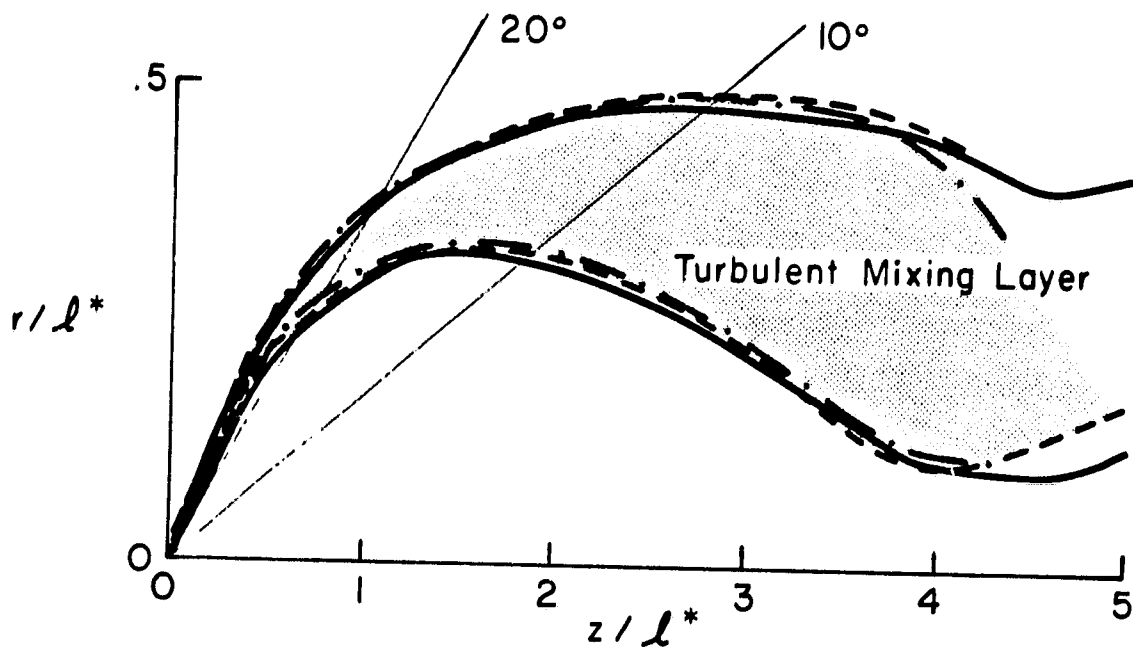60 km, $\ell^* = .153$ km
70 km, $\ell^* = .274$ km
80 km, $\ell^* = .546$ km

Figure 4. Scaled Plume Shapes of Equivalent Shuttle Plume at 60, 70, and 80 km Altitude ($\ell^* = (T/q_\infty)^{1/2}$).

It is important to note that when the electron number density is small ($n_e \leqslant 10^{14}$ m^{-3}), such that the plasma frequency is small compared to the radar frequency, ν ($\nu_p \ll 416.5$ MHz), and the electron-neutral collision frequency is also small compared to ν ($\nu_{en} \ll 2\pi\nu$), the absorption is very weak. For these conditions, the attenuation constant α, is (see Appendix A)

$$\alpha = \frac{8.69}{2} k \left(\frac{\omega_p}{\omega}\right)^2 \left(\frac{\nu_{en}}{\omega}\right) \quad \text{(dB)} \tag{1}$$

Also, the phase constant β,

$$\beta = k \left[1 - \left(\frac{\omega_p}{\omega}\right)^2\right] \simeq k \tag{2}$$

remains the same as the free space wavenumber $k = 2\pi/\lambda$. Since $\omega_p^2 \sim n_e = \mu_e n$, and $\nu_{en} \sim n$, the important result is that

$$\alpha \sim k\mu_e n^2 \sim k\mu_e \rho^2 \tag{3}$$

in the plume. Furthermore, since the chemical composition is frozen, the mole fraction of electrons at any point is proportional to the value of μ_e at the exit plane. This is an important scaling that will be applied to extend the detailed plume predictions to higher altitudes.

The additional attenuating mechanism that occurs when free electrons are present in turbulent flow is scattering by the fluctuating concentration (Tatarski, 1961). This mechanism is also included in PRFIC. For a low density plume, and for large turbulent length scales, Λ, the attenuation due to this mechanism depends on concentration according to (see Appendix A)

$$\alpha_s \sim \Lambda n_e^2/k^2 \sim \Lambda \mu_e^2 \rho^2/k^2 \tag{4}$$

These two mechanisms, absorption and scattering, can be of comparable magnitude in the turbulent shear layer.

3.4 Specific Predictions

Predictions of the attenuation at 416.5 MHz using the detailed numerical flowfield solutions at 60, 70, and 80 km altitude were made with PRFIC. It was necessary to assume that there was a trace amount of contaminant in the exhaust gases. A very small amount, 1 ppm of sodium, was chosen. Sodium has an ionization potential of 5.12 eV. The same results apply to other elements such as K (4.32 eV) and calcium (6.09 eV). In fact, the same result holds even for metals such as Al (5.96 eV), Cr (6.74 eV), Fe (7.83 eV), Ni (7.61 eV), and Cu (7.69 eV). Metal impurities are a potential source from erosion of the thrust chamber.

An impurity level of 1 ppm of any of these elements corresponds to a mass flow of about 1 gm/sec per engine and represents about 1 kg of mass loss for the duration of the main engine burn. This mass loss is larger than that expected for erosion of metal in the engines. A more plausible source is an impurity in the fuel or oxidizer for which the combined flow rate is about 475 kg/sec per engine.

Attenuation, in dB, for the aspect angles of interest at 60 and 80 km altitude is shown in Figure 5. It is possible to match the magnitude of the observed attenuation at these altitudes with the predictions assuming less that 1 ppm of Na, or comparable amounts of other low ionization potential contaminants in the exhaust.

Predictions of the attenuation due to plume absorption and scattering throughout the trajectory were made in the following manner. The magnitude and aspect angle dependence of the attenuation at altitudes higher than 80 km were taken to be the same as that from the detailed numerical solution at 80 km. Arguments based on an approximate density distribution in the plume given in Appendix B suggest that for the mechanism of attenuation by absorption, the magnitude and aspect angle dependence are independent of altitude and vehicle velocity. Predictions of attenuation due to absorption in the plume are then essentially a constant throughout the period of interest except for the changes in effective aspect angle of the line-of-sight through the plume.

The detailed predictions through the plume include a contribution from scattering in the turbulent shear layer. However, that contribution also scales like the absorption if the chemistry is frozen (i.e., $\mu_e^2\rho^2$ and $\mu_e\rho^2$, respectively) except that the scattering includes a normalized electron
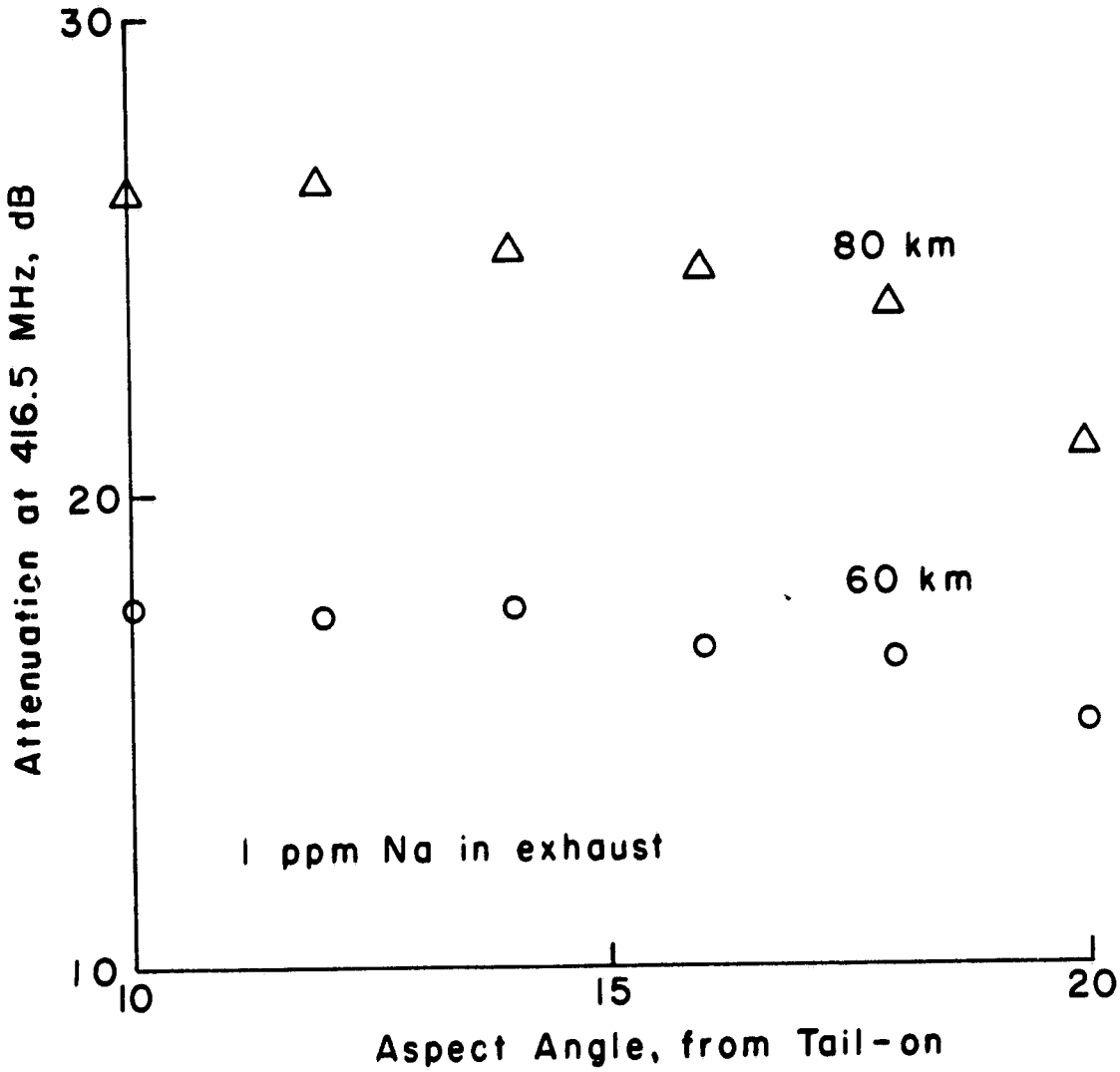
13

Figure 5. Aspect Angle Attenuation for Near Tail-on Transmission
through the Shuttle Plume.

density fluctuation and a length scale. These additional quantities may have some altitude dependence. For example, the turbulent length scale dependence is $\Lambda \sim \ell^* \sim q_\infty^{-1/2}$. Therefore, the actual attenuation through the plume is not strictly independent of altitude or velocity because of the scattering mechanism. Fortunately, the scattering contribution is not a major part of the total attenuation, and any altitude dependence from that mechanism is ignored for the lines-of-sight considered here.

The locations of the RSS antennas on the ET are shown in Figures 6 and 7. They are at diametrically opposed positions on the forward portion of the ET. Coordinates of the two locations in the Orbiter coordinate system (Figure 6) are listed below. The axial location $(X-X_0)$ is the distance forward of the main engine nozzle exit planes. Calculations of the attenuation were made for the antenna location nearest the Orbiter.

Antenna Coordinates

Antenna	Y_0, m	Z_0, m	$X-X_0$, m
Nearest to Orbiter	-2.80	-5.41	42.7
Farthest from Orbiter	2.80	-12.21	42.7

During the portion of the trajectory of interest, the Orbiter is inverted. The antenna nearest to the Orbiter is one with the non-obstructed, line-of-sight to the Cape Command (except for the intervening exhaust plume).

It is important to note that the true line-of-sight through the plume does not pass through the plume axis because of the location of the antenna. A precise description of the line-of-sight direction requires more than a single aspect angle. The calculations given here account for the detailed location of the antenna and line-of-sight. However, for simplicity, the angle of the line-of-sight from the plume axis, ϕ, is used to identify the different lines-of-sight along the trajectory.

The calculation at 80 km was scaled to match the average level of attenuation (about 10 dB) for STS-2. This same nominal level was used for STS-3 and 4. This nominal level corresponds to about 0.5 ppm of trace impurity. Predictions using this nominal level, and accounting for the varying aspect angle along the trajectory, are compared with measurements for STS-2, 3, and 4 in Figure 8. The measured attenuation was taken to be the difference between measurements and NASA predictions for transmission to the
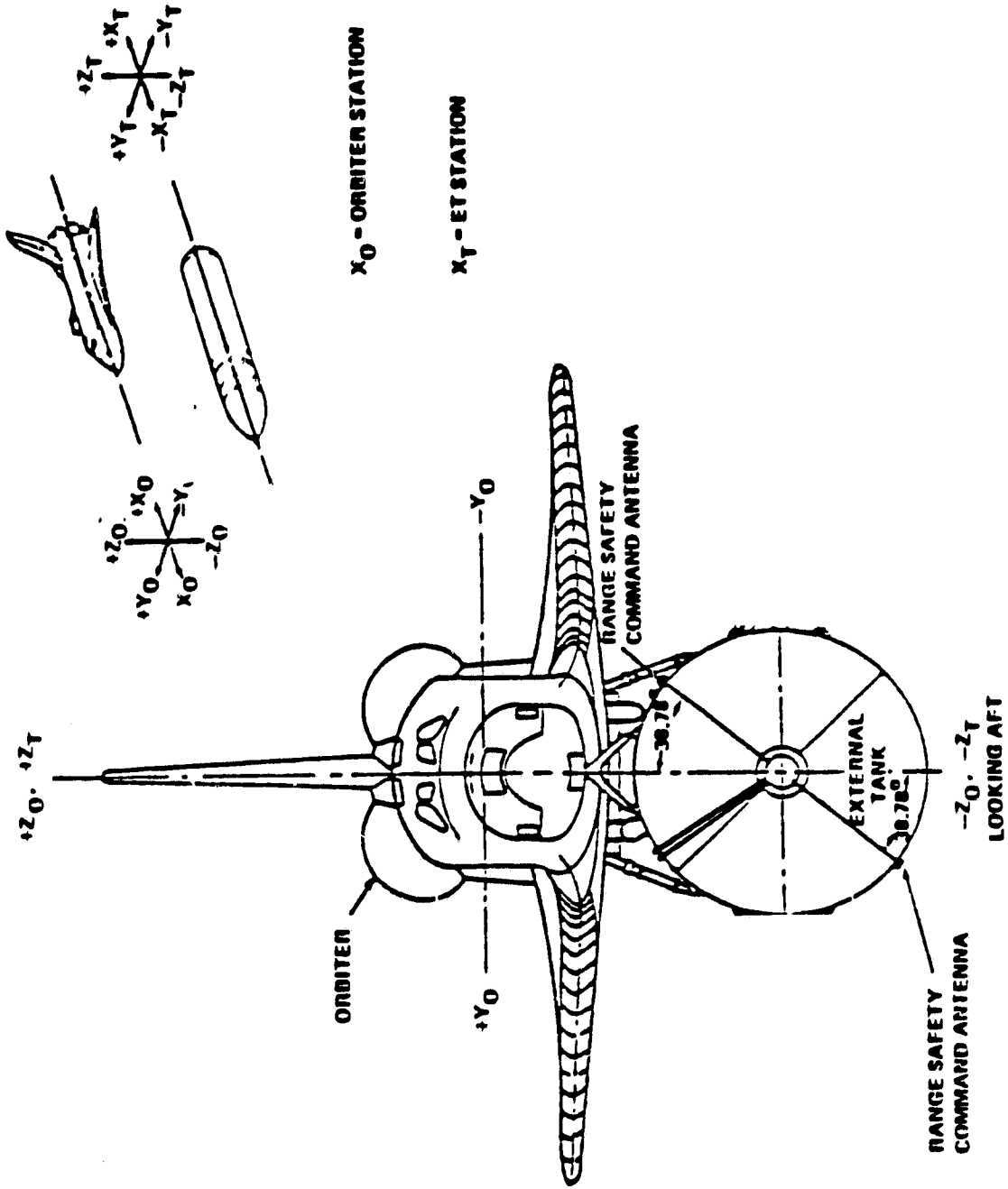
Figure 6. Locations of RS Command Antenna on External Tank (End View).
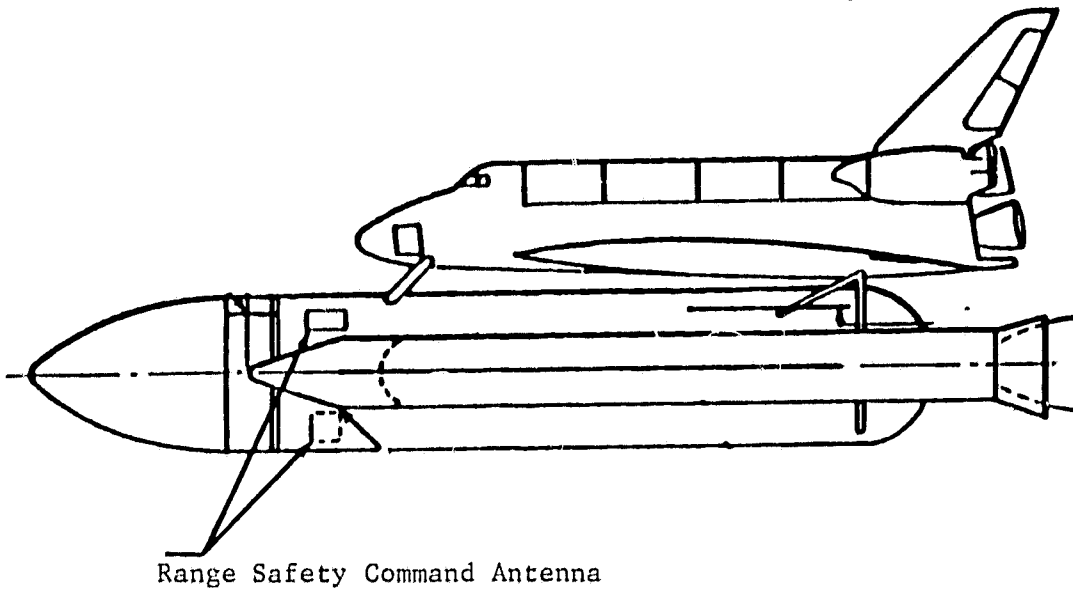
Range Safety Command Antenna

Figure 7. Locations of RS Command Antenna on External Tank
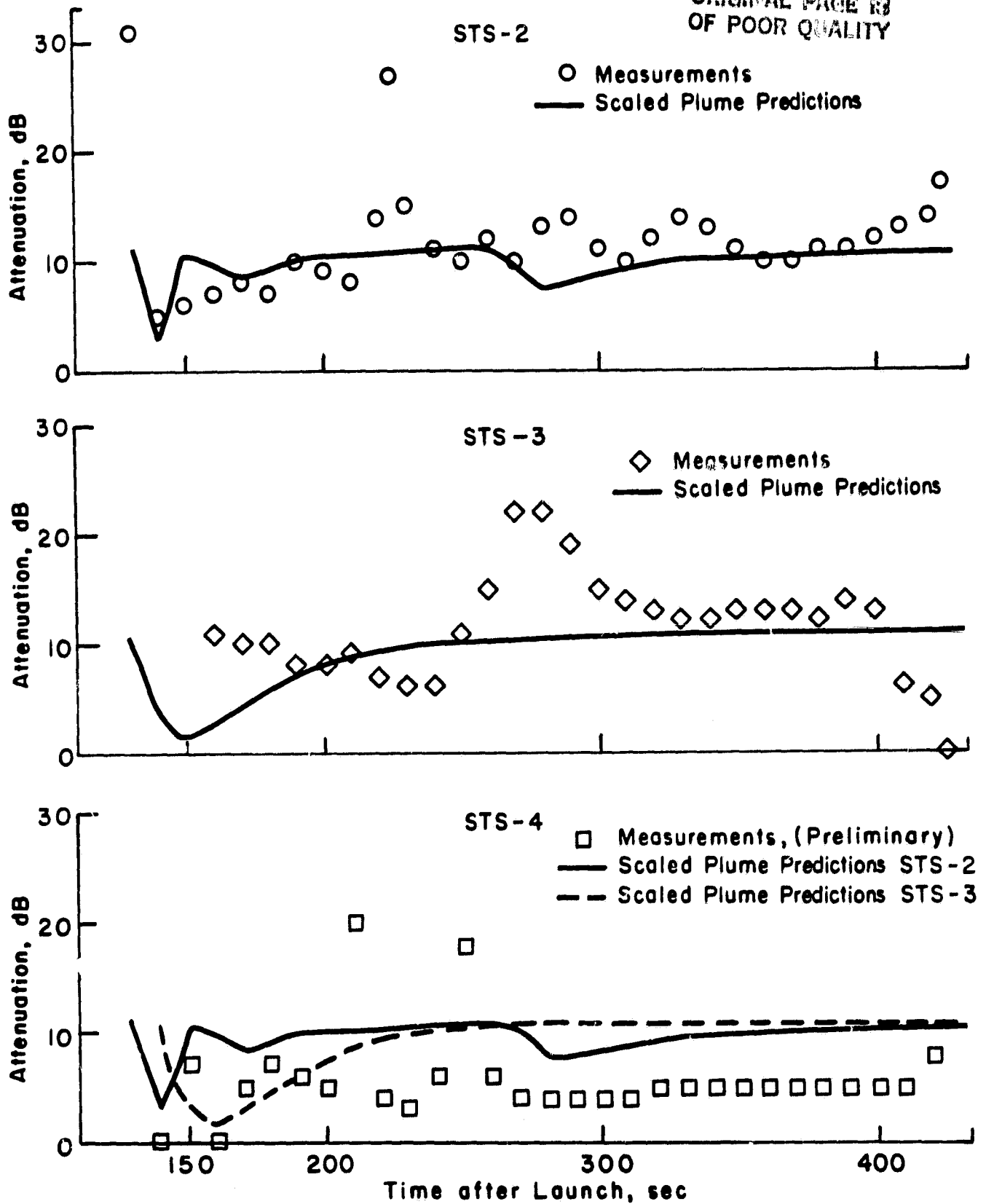(Side View, SRB's are not present beyond ∿ 127 sec).

Figure 8.   Comparison of Observed and Scaled Predictions of Plume
Attenuation for STS-2, 3, and 4.

RSS antenna, using the best estimate of the trajectory (BET) and not accounting for attenuation by the plumes. A complete history of the aspect angles for STS-4 was not available, and so the predictions for STS-2 and 3 are shown.

This comparison suggests that the overall level of attenuation can be explained by the presence of a contaminant in the main engines exhaust that results in absorption by the inviscid core of the plume. The contaminant concentration need be only about 0.5 ppm of a low ionization potential (6 eV or less). There are times when the attenuation substantially exceeds the nominal levels predicted, for example, at 225 sec for STS-2, 270 sec for STS-3, and at 210 and 250 sec for STS-4. These short time increases are not directly explained by the plume absorption. There were no sudden changes in the vehicle attitude or other factors observable in the trajectory data. There are sudden changes in the aspect angle, for example at 135 and 265 sec in STS-2 (Figure 1). However, these times do not coincide with the large increase in attenuation. The same conclusion holds for STS-3.

It is concluded that a trace impurity with a concentration of less than 1 ppm in the main engine oxidizer or fuel can explain the observed attenuation over most of the trajectory between SRB separation and hand over to Bermuda. There are short periods of duration of 20-50 seconds during the trajectory between 200 and 300 seconds where the attenuation exceeds the nominal levels expected for the indicated lines-of-sight. There were no sudden changes in vehicle attitude during these times to indicate a change in the line-of-sight. The plume attenuation based on the single equivalent plume model used here cannot explain these short period increases. In addition, the measurements for STS-4 indicate about half the attenuation reported for STS-2 and STS-3, although the overall trajectory dependence is similar. Since the aspect angles are indicated to be the same for these flights, there is no explanation for this difference, except that the contamination level might have been less for this flight.

There are at least two reasons why there might be short time fluctuations in the observed attenuation. One is related to the exhaust plume/wake structure itself. The actual plume/wake flowfield structure is very complicated because of the multiple engines and complicated body geometry. It is expected that the plume and wake will show some very localized nearfield structure that the single equivalent axisymmetric plume models can not duplicate. It is reasonable to expect that there will be some localized

19

variability in the attenuation as the line-of-sight moves across these non-uniform regions of the flow. A second possibility is that the transmitter line-of-sight may also traverse segments of the exhaust plume that are drifting far behind the vehicle. These segments could be from the main engines or even the SRB's. The times and the additional attenuation contributed by this source would depend on the direction and velocity of the winds at lower altitudes. One or both of these additional features of the exhaust plume structure and ambient conditions could be the reason for the additional attenuation.

4.0 ATTENUATION BY THE WAKE AND SHOCK LAYER

4.1 Sources Ionizable Species

Unlike the exhaust plume, which required an assumed source of ionizable species, the Orbiter wake and shock layer contain two known sources of electrons. One is from the ablation products leaving the Orbiter and ET thermal protection system, and the other is from the ionization of air by the vehicle shock waves.
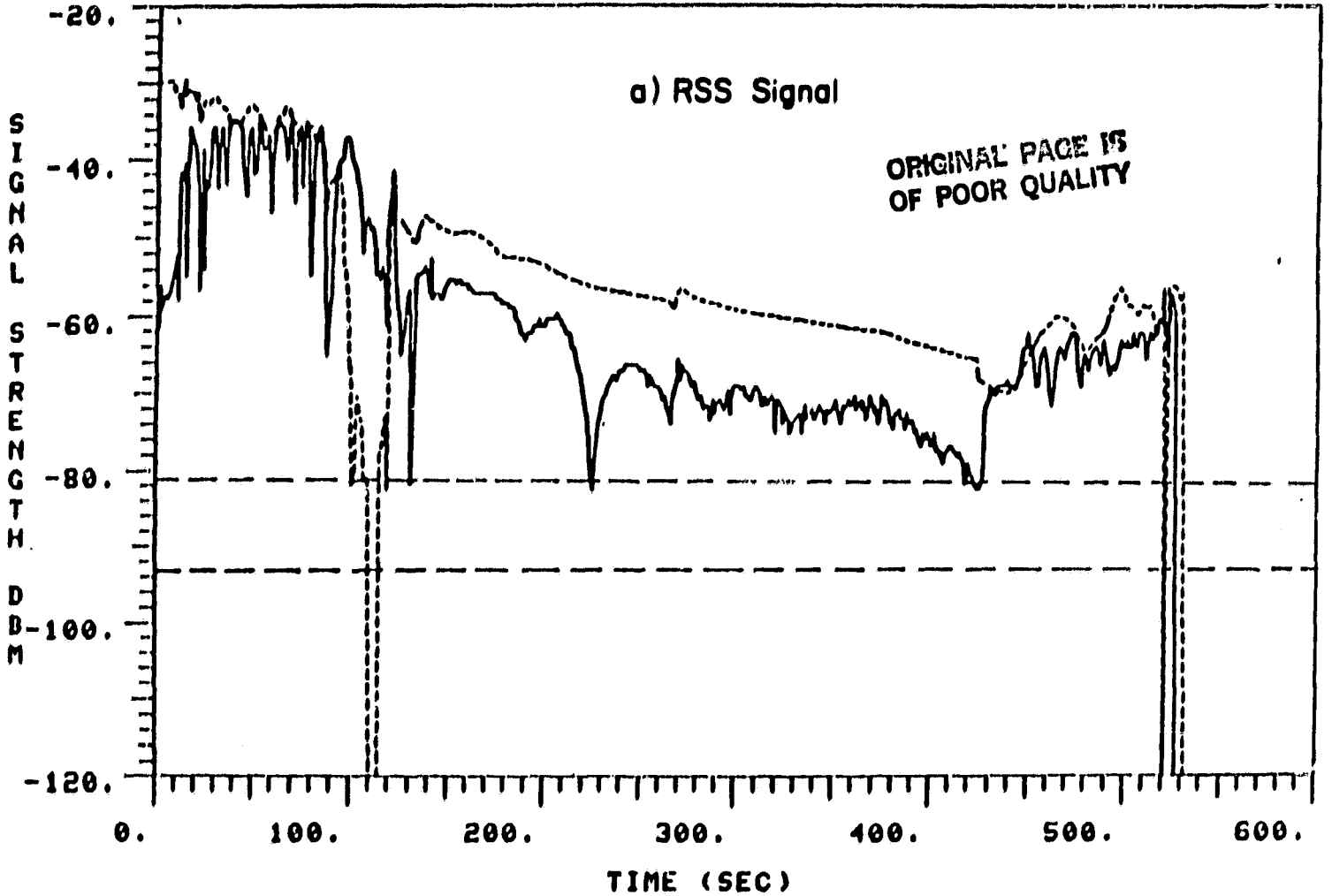
4.2 Attenuation by Ablation Products

The ET ablation products contain Na, K, and Ca and consequently, are possibly ionized in the mixing layer between plume and wake. However, the duration of ablation is confined to a short period after SRB separation. Heating rates are not sufficiently severe to maintain any significant ablation at the higher altitudes. The duration of the primary ablation is compared with the attenuation in Figure 9. The known ablation is over by 200 sec into the trajectory. More importantly, the measured attenuation during the ablation period shows no time dependence like the ablation rate. If ablation was a primary contributor, the attenuation should show some time dependence that would correlate with the rate of ablation. It is concluded that the ET heat shield ablation is an unlikely contributor to the attenuation.

4.3 Shocked Ionized Air

The second source of electrons, the vehicle shock layer, is velocity dependent. For the relatively slow (compared to unmanned boosters) Shuttle Orbiter, which does not exceed a flight Mach number of seven until about 250 sec and 113 km altitude, the ionization behind the shock is very low level. The initial electron number density behind a shock in clean air does

20

a) RSS Signal

ORIGINAL PAGE IS
OF POOR QUALITY

SIGNAL STRENGTH DBM

TIME (SEC)

FILE   : STS2PWR   _____ ET
ABSCISSA : TIME   ------- Composite Predicted Data

RECEIVED SIGNAL STRENGTH VS TIME

b) ET Ablation Rate

TOTAL ABLATION RATE (LB/SEC)

TIME (SEC)

ARAP 82-2200

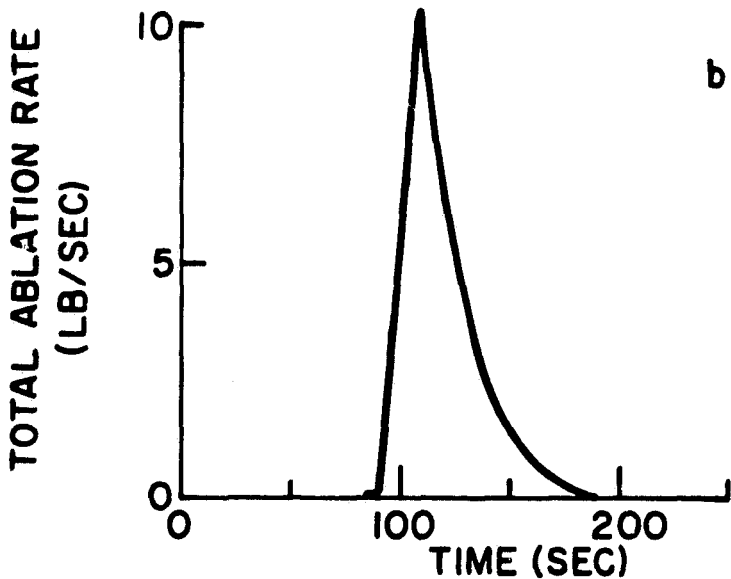Figure 9. Comparison of Time Dependence
of External Tank Ablation
Rate and Attenuation for
STS-2.

not reach levels adequate to explain the observed attenuation until a velocity of about 2.8 km/sec ($M_\infty = 7.2$) at a time of 240 sec and altitude of 110 km. At this point, the number density becomes comparable to those initial levels in the exhaust plume needed to give the correct attenuation levels. However, a more important consideration is that in the shear layer, attenuation by the turbulent scattering is more important than absorption. According to the earlier analysis, scattering scales with the square of electron mole fraction

$$\alpha_s \sim \mu_e^2 \rho^2 \Lambda/k^2 \tag{5}$$

while absorption scales linearly with mole fraction

$$\alpha \sim k\mu_e \rho^2 \qquad \text{ORIGINAL PAGE IS} \tag{6}$$
$$\text{OF POOR QUALITY}$$

Predictions of attenuation from this source, scaled from the lower altitude results according to Eq. (5), and using equilibrium number densities behind the shock at the appropriate altitude and flight velocity, were made. The magnitude and altitude dependence (because of the μ_e^2 dependence) is sufficiently different from that observed that this source of attenuation is not a likely source. This mechanism could become important at higher velocities, however, if the transmitter of the RSS signal is maintained near the launch site longer into the trajectory.

5.0 ADDITIONAL ATTENUATION MECHANISMS

5.1 Absorption by Water Vapor

It is well-known that microwave radiation is absorbed by the rotational transitions of water vapor and other heteronuclear polyatomic molecules. Since the exhaust plume is predominantly water vapor (73 percent mole fraction), this is a potential explanation. In addition, this absorption would be altitude independent, like that found for the attenuation by free electrons.

An upper bound estimate of this absorption is easily made. The maximum attenuation will occur along the plume axis. If the plume density distribution described in Appendix B is used, the attenuation due to absorption by water vapor will always be less than the quantity

$$\int \alpha_{H_2O} ds = \int \alpha_o \frac{\mu_{H_2O}}{\mu_o} \frac{n}{n_o} ds < \alpha_o \frac{\mu_{H_2O}}{\mu_o} \frac{n_c}{n_o} \int_0^\infty \frac{n_{CL}}{n_c} dr \qquad (7)$$

$$= \alpha_o \frac{\mu_{H_2O}}{\mu_o} \frac{\rho_c}{\rho_o} \frac{\overline{M}_o}{\overline{M}_c} \int_0^\infty \frac{\rho_{CL}}{\rho_c} dr \qquad (8)$$

$$= \alpha_o \frac{\mu_{H_2O}}{\mu_o} \frac{\rho_c}{\rho_o} \frac{\overline{M}_o}{\overline{M}_c} r^* \pi \left(\frac{B}{\rho_e/\rho_c} \right)^{1/2} . \qquad (9)$$

α_o is the absorption coefficient at the reference conditions given by Hill and Clifford (1981); $\alpha_o = 10^{-7}$ M^{-1} at 416.5 MHz ($\omega = 1/\lambda$ .0139 cm^{-1}), $\mu_o = .0278$, mixture molecular weight, $M_o = 28$, $T_o = 300$ K, $p_o = 1$ atm. For the main engine plume, $\overline{M} = 13.603$ $r^* = 0.2235$ m (effective value), $\mu_{H_2O} = 0.727$, $\rho_c/\rho_o = 8.26$, $\rho_e/\rho_c = 2.75 \times 10^{-3}$, and $B = .206$.

$$\int \alpha_{H_2O} ds < 2.70 \times 10^{-4} = .00235 \text{ dB} \qquad (10)$$

This result suggests that the absorption by water vapor is unimportant.

There are uncertainties in this estimate. One uncertainty concerns the absence of rotational lines that become important at higher temperatures than that for which the line atlas used to predict α_o was compiled (Hill and Clifford, 1981). It is not expected that this could increase the absorption estimate by more than a factor of 10^3, which would be required for this mechanism to be important.

5.2 Reflection by Weakly Ionized Layer

The wave front from the Cape Command transmitter must penetrate the weakly ionized shock layer and plume in order to reach the antenna. It is known that some energy is reflected as a wave traverses a discontinuity in optical properties. This mechanism would still require some trace impurity in the plume, but the basic physical mechanism of removing energy from the wave propagating to the antenna is different from absorption. A suggestion of the importance of this effect can be obtained from a simple solution for reflection of a wave incident at angle θ to a plane ionized homogeneous layer (Taylor, 1961; Panofsky and Phillips, 1962). The amplitude reflection coefficient, R (using the absorption coefficient of Eq. (1)) is

$$R = \frac{\cos\theta - (n_p - \sin^2\theta)^{1/2}}{\cos\theta + (n_p^2 - \sin^2\theta)^{1/2}} \approx \frac{1\alpha}{k\cos^2\theta} = \frac{1}{2}\left(\frac{\omega_p}{\omega}\right)^2\left(\frac{\nu_{en}}{\omega}\right)/\cos^2\theta \qquad (11)$$

for small α. The power reflection coefficient is $|R|^2$, and the attenuation is approximately

$$\int\alpha ds \sim \frac{4.34}{4}\left(\frac{\omega_p}{\omega}\right)^4\left(\frac{\nu_{en}}{\omega}\right)^2 / \cos^4\theta \quad (dB) \qquad (12)$$

for the small values of ω_p/ω and ν_{en}/ω encountered in the plume. In the outer edges of the shear layer, $\alpha < 10^{-3}$ m^{-1}. For 416.5 MHz, $k = 8.727$ m^{-1}

$$\int\alpha ds < 0.15 \text{ dB}$$

even for grazing incidence ($\theta = 89°$). Reflection is therefore not a likely explanation for the observed attenuation.

5.3 Scattering by Turbulent Fluctuations in Index of Refraction

Scattering by bound electrons (fluctuations in the real part of the index of refraction, n_p) can occur as well as that due to fluctuations in a free electron concentration. This is the phenomena that is responsible for scintillation of starlight at visible wavelengths. It is caused by fluctuations in the index of refraction due to temperature and species concentration fluctuations. Like the scattering by free electrons, the total energy in the beam remains unaltered (in the absence of absorption) but is scattered out of the direction of propagation. For this mechanism, the effective attenuation is given by

$$\int\alpha ds = 8.48 \ k^2 \int_0^s \frac{\overline{n'^2}}{2} \Lambda ds \qquad (dB) \qquad (13)$$

$\overline{n'^2}$ is the mean square index of refraction fluctuation and Λ is the turbulence macroscale. The primary contribution to $\overline{n'^2}$ is from the temperature fluctuations in the turbulent mixing layer at the plume boundary. For typical cases, $\overline{n'^2} < 10^{-14}$, $\Lambda = 10$-100 m, and

$$\int\alpha ds < 10^{-8} \text{ dB} \qquad (14)$$

24

This estimate suggests that the scintillation mechanism is too weak to contribute any attenuation.

6.0 SUMMARY AND CONCLUSIONS

An analysis of the possible mechanisms responsible for attenuation of the Space Shuttle Range Safety System command signal at 416.5 MHz between SRB separation and hand over to Bermuda is summarized. During this period, the line-of-sight from the Cape Command Center to the antenna on the external tank passes through the exhaust plumes of the Orbiter main engines. This attenuation was observed on all STS flights for which the necessary measurements were recorded (all except STS-1). The following mechanisms were examined:

1. absorption and scattering by the exhaust plume flow, assuming a trace amount of easily ionizable impurity in the main engine exhaust

2. absorption and scattering from the outer edges of the plume and vehicle wake due to free electrons added by the external tank ablation products and ionization of clear air by the vehicle and plume shock waves

3. absorption by rotational lines of water vapor in the plumes

4. reflection of the incident wave by the edges of the plume

5. attenuation by scattering from fluctuations in the index of refraction in the turbulent mixing layer of the plume.

The only mechanism that yields the correct magnitude, and altitude and aspect angle dependence, is absorption by the exhaust plume. However, it is necessary to assume about 0.5 ppm of an easily ionizable impurity species in the exhaust for this mechanism to be present. Any species with an ionization potential of about 6 eV or less would be adequate. With this assumption, it is possible to predict the correct level of attenuation. This source of attenuation is predicted to have no velocity or altitude dependence, but it does depend on aspect angle. The overall dependence of the observed attenuation during the trajectory is reproduced, except for short period increases. It is suggested that these features may be due to either detailed structure in the plume/wake that was not modeled or to temporary obscuration by drifting elements of the plume far downstream from the vehicle.

REFERENCES

Boynton, F.P., et al.: Range Safety Signal Propagation through the SRM Exhaust Plume of the Space Shuttle. PD-B-77-141, Physical Dynamics, Inc., Calif., May 1977.

Boynton, F.P.; Rajasekhar, P.S.: Plume RF Interference Calculations for Space Shuttle. PD-B-78-175, May 1978.

Dash, S.M., et al.: Operating Instructions for a Preliminary Version of the JANNAF Standard Plume Flowfield Model (SPF/1). A.R.A.P. Report No. 415, Aeronautical Research Associates of Princeton, Inc., N.J., June 1980.

Gordon, S.; McBride, B.J.: Computer Program for Calculation of Complex Chemical Equilibrium Compositions, Rocket Performance, Incident and Reflected Shocks, and Chapman-Jouguet Detonations. NASA SP-273, March 1976.

Hill, J.A.F.; Draper, J.S.: Analytical Approximation for the Flow from a Nozzle into a Vacuum. Journal of Spacecraft, vol. 3, no. 10, 1966, pp. 1552-1554.

Hill, R.J.; Clifford, S.F.: Contribution of Water Vapor Monomer Resonances to Fluctuations of Refraction and Absorption for Submillimeter through Centimeter Wavelengths. Radio Science, vol. 16, no. 1, 1981, pp. 77-82.

Lee, R.H.C.; Chang, I-S.; Stewart, G.E.: Studies of Plasma Properties in Rocket Plumes. The Aerospace Corp., SD-TR-82-44, prepared for Space Division, Air Force Systems Command, Calif., May 1982.

Mitchner, M.; Kruger, C.H.; Partially Ionized Gases. John Wiley and Sons (N.Y.), 1973, pp. 156-161.

Moran, J.P.: Mixing Layers for Highly Underexpanded Supersonic Jets in Hypersonic Streams. Journal of Fluid Mechanics, vol. 65, part 1, 1974, pp. 153-175.

Panofsky, W.K.H.; Phillips, M.: Classical Electricity and Magnetism. Addison-Wesely (Mass.), 1962, chapter 11.

Pearce R.E.; McCullough, R.W.: The Naval Weapons Center Plume Radar Frequency Interference Code. A.R.A.P. Report No. . Also NWC TP 6386, prepared for Naval Weapons Center, China Lake, Calif., September 1982.

Tatarski, V.I. (R.A. Silverman, transl.): Wave Propagation in a Turbulent Medium, McGraw-Hill (N.Y.), 1961, chapter 4.

Taylor, L.S.: RF Reflectance of Plasma Sheaths. Proceedings of the IRE, December 1961, pp. 1831-1836.

APPENDIX A: Absorption and Scattering in a Weakly Ionized, Low Density Gas

If an electromagnetic wave is assumed to have a spatial dependence on distance, x, along the direction of propagation of the form

$$E \sim \exp(ikx) \tag{A-1}$$

in an ionized gas, then the dispersion relation is (Mitchner and Kruger, 1973)

$$\left(\frac{k\omega}{c}\right)^2 = 1 - \frac{\left(\frac{\omega_p}{\omega}\right)^2}{1 + \left(\frac{\nu_{en}}{\omega}\right)^2} + i\,\frac{\left(\frac{\omega_p}{\omega}\right)^2 \left(\frac{\nu_{en}}{\omega}\right)}{1 + \left(\frac{\nu_{en}}{\omega}\right)^2} \,. \tag{A-2}$$

$k\omega/c = n_p$ is the index of refraction of the plasma which is generally complex. The real part is the usual refractive index (ratio of speed of light in a vacuum to that in the plasma), and the imaginary part is the absorption index, which accounts for the attenuation of wave amplitude. If

$$\left(\frac{k\omega}{c}\right)^2 = K_R + i\,K_I \tag{A-3}$$

then

$$\mathrm{Re}\left(\frac{k\omega}{c}\right) = \beta = \frac{\omega}{c}\left\{\frac{|K| + K_R}{2}\right\}^{1/2} \tag{A-4}$$

$$\mathrm{Im}\left(\frac{k\omega}{c}\right) = \alpha = \frac{\omega}{c}\left\{\frac{|K| - K_R}{2}\right\}^{1/2} \tag{A-5}$$

In the special case of a weakly ionized gas (like the Shuttle main engine with a trace impurity, or the vehicle and plume shock layer)

$$\frac{\omega_p}{\omega} \ll 1 \tag{A-6}$$

Furthermore, for low density flows ($\nu_{en} = \nu_e nQ$, where n is the particle number density $\sim p/T$, ν_e is the electron thermal velocity $\sim T^{1/2}$, and Q is a collision cross-section $\simeq 1.5 \times 10^{-19}$ m^2)

$$\frac{\nu_{en}}{\omega} \ll 1 \qquad (A\text{-}7)$$

With these two approximations, (Pearce and McCullough, 1982)

$$\alpha = \frac{1}{2} k \left(\frac{\omega_p}{\omega}\right)^2 \left(\frac{\nu_{en}}{\omega}\right) \qquad (A\text{-}8)$$

and

$$\beta = k \quad . \qquad (A\text{-}9)$$

In an ionized turbulent flow, the number density of free electrons fluctuate (due to fluctuations in temperature, pressure, and species concentrations). These fluctuations create locally non-homogeneous regions (eddies) of non-uniform refractive index that act to scatter the RF wave. Various models for the scattering from these turbulent non-homogeneous regions have been developed (Tatarski, 1961). Scattering does not reduce the overall energy in the RF radiation, however, it removes it from the direction of propagation and can therefore contribute an apparent attenuation. The effective attenuation coefficient due to this scattering is

$$\alpha_s = .0528(8\pi^3) \left(\frac{\overline{n_e'^2}}{\overline{n_e^2}}\right) \frac{\overline{n_e^2} \, r_t^2 \, \Lambda^3}{\left[1 + \left(\frac{\nu_{en}}{\omega}\right)^2\right]^2} Q(2k^2\Lambda^2) \qquad (A\text{-}10)$$

$\overline{n_e'^2}/\overline{n_e^2}$ is the mean square fluctuation of electron number density normalized by the square of the mean number density, r_t^2 is the Thompson radius of the electron (2.81×10^{-15} m^2), Λ is the turbulence macroscale, and Q is a scattering efficiency. For the Shuttle main engine and 416.5 MHz radiation, $2k^2\Lambda^2$ is large (Pearce and McCullough, 1982),

$$Q \to \frac{12\pi}{5(2k^2\Lambda^2)} \qquad (A\text{-}11)$$

and the attenuation due to scattering has the dependence

$$\alpha_s \sim \left(\frac{\overline{n_e'^2}}{\overline{n_e^2}}\right) \overline{n_e^2} \, \Lambda/k^2 \quad . \qquad (A\text{-}12)$$

APPENDIX B: Approximate Aspect Angle and Altitude Dependence of Attenuation through the Exhaust plume

As indicated in the main section of the report, the attenuation through the core region of the plume depends on the integral of the square of the plume density along the line-of-sight.

$$\int_0^S \alpha \, ds \sim \int_0^S \rho^2 \, ds \tag{B-1}$$

This appendix summarizes the derivation of an approximate value for this integral and more importantly, suggests the altitude and aspect angle dependence of the expected attenuation at altitudes beyond the capability of the detailed numerical solutions.

For this purpose, an approximate density distribution in the plume proposed by Hill and Draper (1966) is used.

$$\frac{\rho}{\rho_c} = 4B \frac{r^{*2}}{r^2} \exp - \left(\Lambda^2 \beta^3 \right) \tag{B-2}$$

This is a non-uniform spherical source flow model which separates the radial (r) dependence from the angular dependence, $\beta = 1 - \cos\phi$, where ϕ is the angle between the radial direction and axis of symmetry ($\pi-\phi$ is the aspect angle of the line-of-sight). B and Λ are constants depending on the motor thrust and specific heat ratio. This and similar models have been widely used and tested in many plume analyses (Moran, 1974; Lee, et al., 1982).

This density relation will be used to evaluate the integral in Eq. (1) along a line-of-sight with fixed ϕ to approximate that of the line-of-sight between Cape Command and the RSS antenna on the ET. The line-of-sight does not actually follow along a radial ray from the nozzle exit, but it is very nearly that on a plume scale defined by $\ell*$.

First, it is necessary to modify the density distribution near the origin. To accomplish this, a curve fit between the exit plane density ρ_e/ρ_c and the asymptotic radial decay rate

$$\lim_{r \to \infty} \frac{\rho}{\rho_c} \sim r^*/r^2 \tag{B-3}$$

29

is used. A satisfactory form is

$$\frac{\rho}{\rho_c} = \frac{\rho_e/\rho_c}{1 + \frac{\rho_e/\rho_c}{4Br*^2} r^2} \tag{B-4}$$

The density at any point in the plume is then given by

$$\frac{\rho}{\rho_c} = \frac{\rho_e/\rho_c \exp - \Lambda^2\beta^2}{1 + \frac{\rho_e/\rho_c}{4Br*^2} r^2} \tag{B-5}$$

For a fixed radial angle ϕ, the attenuation through the plume is proportional to

$$\int \alpha ds \sim \left(\frac{\rho_e}{\rho_c}\right)^2 \exp(-2\Lambda^2\beta^2) \int_0^\infty \frac{dr}{\left[1 + \frac{\rho_e/\rho_c}{4Br*^2} r^2\right]^2} \tag{B-6}$$

$$= \left(\frac{\rho_e}{\rho_c}\right)^{3/2} \exp\left(-2\Lambda^2\beta^2\right) r* \frac{\pi}{2} \sqrt{B} \tag{B-7}$$

Since Λ and B are independent of altitude, this approximation indicates that the attenuation due to absorption by free electrons in a high altitude exhaust plume of chemically frozen composition is essentially independent of altitude. It does depend on aspect angle ($\pi-\phi$). A search for that dependence is the motivation for using this approximation model to extend the more detailed calculations to higher altitudes.

Since all parameters except Λ and β do not affect the angular dependence of the attenuation, only these need be varied to answer the question of the aspect angle sensitivity. Λ depends on the vacuum and maximum thrust coefficients (Moran, 1974)

$$\Lambda = 1/\sqrt{\pi} \left(1 - C_F/C_{F_m}\right) \tag{B-8}$$

For the main engine, $C_F = 1.960$, $C_{F_m} = 2.134$, and $\Lambda = 6.909$. The attenuation relative to that at $\phi = 10°$, predicted by this simple model, is compared to the detailed numerical integration through the plume at an altitude of 80 km

in Table B-1.

Table B-1. Aspect Angle Dependence of Attenuation
through the Plume

(normalized by attenuation at $\phi = 10^{\circ}$)

ϕ, deg	Eq. (7)	Detailed Predictions at 80 km Altitude
12	0.977	1.005
16	0.867	0.936
20	0.722	0.794
24	0.501	0.611

Both the simple model and precise calculation show a 20-30 percent
decrease in attenuation as the aspect $(\pi-\phi)$ decreases from near tail-on.
Moreover, since the approximate model has no altitude dependence and becomes a
more accurate approximation to the actual plume as the altitude increases, it
is argued that the aspect angle dependence and magnitude of attenuation are
independent of altitude.